Comprehensive Analysis of mRNAs and miRNAs in the Ovarian Follicles of Uniparous and Multiple Goats at Estrus Phase

Xian Zou
South China Agricultural Univeersity College of Animal Science; Guangdong Academy of Agricultural Sciences Institute of Animal Science

Tingting Lu (18819255207@163.com)
South China Agricultural University College of Animal Science https://orcid.org/0000-0002-3140-5882

Zhifeng Zhao
South China Agricultural University College of Animal Science

Guangbin Liu
South China Agricultural University College of Animal Science

Zhiquan Lian
South China Agricultural University College of Animal Science

Yongqing Guo
South China Agricultural University College of Animal Science

Baoli Sun
South China Agricultural University College of Animal Science

Dewu Liu
South China Agricultural University College of Animal Science

Yaokun Li
South China Agricultural University College of Animal Science

Research article

Keywords: Goat, Ovarian Follicles, mRNAs, miRNAs, Kidding rate, Ovulation rate, RNA-seq

Posted Date: October 10th, 2019

DOI: https://doi.org/10.21203/rs.2.15819/v1

Version of Record: A version of this preprint was published on March 30th, 2020. See the published version at https://doi.org/10.1186/s12864-020-6671-4.

Abstract

Background

Fertility is an important economic trait in production of meat goat, and follicular development plays an important role in fertility. Despite many mRNAs and microRNAs (miRNAs) have been found in playing critical roles in ovarian biological processes, the interactions between mRNAs and miRNAs in follicular development is not yet completely understood. In addition, less attention has been given to the single follicle (dominant or atretic follicle) in goat. The study was aimed to identify mRNAs, miRNAs and signaling pathways as well as their interaction networks in the ovarian follicles (large follicles and small follicles) of multiple and uniparous goats (Chuanzhong Black Goats) at estrus phase by using a deep RNA-sequencing (RNA-seq) method.

Results

The result showed that there were more large follicles in multiple than in uniparous goats ($P < 0.05$), while no difference was observed in small follicles between them ($P > 0.05$). For the small follicles of multiple and uniparous goats at estrus phase, 289 differentially expressed mRNAs (DEmRNAs) and 16 DEmiRNAs were identified; and for the large follicles, 195 DEmRNAs and 7 DEmiRNAs were identified. Ovarian steroidogenesis and steroid hormone biosynthesis were significantly enriched in small follicles, while ABC transporters and steroid hormone biosynthesis in large follicles. The results of qRT-PCR were generally consistent with the RNA-seq data. The mRNA-miRNA interaction network showed that CD36 (miR-122, miR-200a, miR-141), TNFAIP6 (miR-141, miR-200a, miR-182), CYP11A1 (miR-122), SERPINA5 (miR-1, miR-206, miR-133a-3p, miR-133b) and PTGFR (miR-182, miR-122) might be related to fertility, but need further verification.

Conclusion

This study provides the first identification of the DEmRNAs and DEmiRNAs as well as their interactions in the follicles of multiple and uniparous goats at estrus phase by using RNA-seq technology. These analyses provide new clues to uncover molecular mechanisms and signaling networks of goat reproduction which could be potentially used to increase ovulation rate and kidding rate in goat.

Introduction

Ovulation rate is the key factor affecting the kidding rate, which is one of the most important economic traits in goat production [1–3]. However, the genetic mechanism of kidding rate that is associated with ovulation rate is poorly understood, which largely limits the improvement of kidding rate through genetic selection. The major function of the ovary is to produce oocytes for fertilization and secrete steroid hormones for regulating follicular development and control goat oestrus [4]. Oocytes mature in follicles surrounded by nurturing granulosa cells and all are enclosed by a basal lamina [5, 6]. Only 1% of follicles reach ovulation while more than 99% of follicles undergo atresia in mammals [7–11]. Hence, it's

important to study the mechanism to regulate the number of oocytes ovulated and to contribute to the timing of ovulation.

In mammals, studies on follicles were mainly concentrated in zebrafish [12], mice [13], humans [14], pigs [15], bovine [16], rats [17] and sheep [18]. They revealed the effects of granulosa cells and theca cells on follicular development, follicular atresia and luteal development, and further elucidated the mechanism of genes and signaling pathways. However, little was known on goat follicles. In goat, the studies worked to identify the key genes that involved in the regulation of ovulation rate and kidding rate by transcriptome sequencing of goat ovaries, and the signaling pathways that affected ovulation and fertility [1, 4, 19–25]. The study on litter size of goats showed that *PDGFRB, MARCH1, KDM6A, CSN1S1, SIRT3, KITLG, GHR, ATBF1, INHA, GNRH1* and *GDF9* might be candidate genes for goat reproductive traits [22, 26–35]. Growth hormone (GH) and members of the insulin-like growth factors (IGF-I and IGF-II) family system may play a key role in the follicular development and atresia [2, 36], and the genes *FER1L4* and *SRD5A2* may be associated with the high fecundity of goats [37]. In addition, many studies suggested that microRNAs (miRNAs) influenced ovarian biological processes in goat, and a lot of differentially expressed miRNAs (DEmiRNAs) have been identified and comparatively analyzed in the ovaries of prolifc and non-prolifc goats, such as miR–21, miR–99a, miRNA–143, let–7f, miR–493 and miR–200b [1, 25, 38]. However, the major genes and miRNAs related to ovulation rate and litter size have not yet been identified in goats through transcriptome sequencing of ovary as a whole. Because of that the follicle is a unique micro-environment within which the oocyte can develop and mature to a fertilisable gamete, it is very necessary to study the single follicle to explore the factors affecting ovulation rate and kidding rate in goats.

Chuanzhong (CZ) black goat is an excellent local goat resource in China. The resources are abundant in China as well as in Southeast Asia, and play an important role in herbivorous livestock [39]. After long-term natural selection and artificial cultivation, CZ black goat has gradually formed local meat goat breeds with high genetic stability [40]. However, low fecundity was still the main bottleneck restricting the development of high efficiency goat industry.

To better understand the role and importance of follicles in kidding rate, we undertook transcriptome profiling of small follicles (S, diameter (d) <3 mm) and large follicles (d >1 cm) from multiple and uniparous CZ black goats during estrus phase to identify DEmRNA and DEmiRNA, respectively. Furthermore, the mRNA and miRNA interaction networks were built, and Gene Ontology (GO) and Kyoto Encyclopedia of Genes and Genomes (KEGG) enrichment analyses of DEmRNAs and target genes of miRNAs were conducted. The study will further explore the role of ovarian follicular mRNAs and miRNAs in goat reproduction, and provide theoretical basis for improving ovulation and kidding rate in the future.

Result

1. Comparison of follicles between multiple and uniparous in CZ black goat

Among the separated follicles used for sequencing, large follicles (d >1 cm) were larger with abundant blood vessels on the surface, while the small follicles (d <3 mm) were relatively small and had no abundant blood vessels (Figure 1). After separation of follicles, the number of follicles in uniparous and multiple goats was counted and analyzed (Table 1). The total number of follicles in multiple goats was more than that in uniparous goats (P <0.05). Furthermore, there was significant difference in the number of large follicles between multiple and uniparous goats (P <0.05), while no difference in small follicles (P >0.05).

2. Analysis of transcriptome sequencing and mapping

We collected twelve large follicles from four uniparous goats and four multiple goats, and nine small follicular pools from four uniparous goats and five multiple goats. Eight to ten small follicles were pooled from each goat for a replicate, and only one single large follicle from each goat for a replicate. Then we sequenced RNA libraries of these seventeen follicular samples. Counts of clean reads and mapped ratio of sequencing results were displayed in Table 2. The data showed that the sequencing results met the requirements and can be further analyzed. Finally, we obtained four groups to further analysis: Uniparous-small follicles vs Multiple-small follicles (Uni-S vs Mul-S) and Uniparous-large follicles vs Multiple-large follicles (Uni-L vs Mul-L).

3. Identification of DEmRNAs and DEmiRNAs

For small follicles, a total of 289 DEmRNAs (131 upregulated and 158 downregulated) and seven DEmiRNAs (seven downregulated) were indentified in Uni-S vs Mul-S (Figure 2a and Table 3a). For large follicles, a total of 195 DEmRNAs (120 upregulated and 75 downregulated) and 16 DEmiRNAs (4 upregulated and 12 downregulated) were indentified in Uni-L vs Mul-L (Figure 2b and Table 3b). For better analysis, we re-screened DEmRNA based on FPKM> 1 at least three samples of each group. Then, we obtained 119 and 37 DEmRNAs from Uni-S vs Mul-S and Uni-L vs Mul-L, respectively, and the top 10 DEmRNAs and DEmiRNAs were showed in Table 3. The venn diagrams of shared DEmRNAs and DEmiRNAs were showed in Figure 2c-d, 2 shared DEmRNAs (*AMDHD1* and *LOC102190765)* and 5 shared DEmiRNA (miR–141, miR451–5p, miR–122, miR–182 and miR–206) were identified in both Uni-S vs Mul-S and Uni-L vs Mul-L.

4. Functional annotation of DEmRNAs

According to the functional annotation of DEmRNAs between Uni-S and Mul-S, 455 GO terms were significantly enriched including cell periphery, plasma membrane, steroid biosynthetic process, steroid hydroxylase activity, receptor binding (Table 4), and KEGG pathways including ovarian steroidogenesis, cortisol synthesis and secretion, cytokine-cytokine receptor interaction, steroid hormone biosynthesis, metabolism of xenobiotics by cytochrome P450 (Figure 2e).

Based on the functional annotation of DEmRNAs between Uni-L and Mul-L, 322 GO terms were significantly enriched including cell periphery, plasma membrane, animal organ development, embryo

development, anion channel activity (Table 4), and KEGG pathways including ABC transporters, retinol metabolism, steroid hormone biosynthesis, drug metabolism-cytochrome P450, metabolism of xenobiotics by cytochrome P450 (Figure 2f).

5. DEmRNA-DEmiRNA interaction network

For Uni-S vs Mul-S, a total of 76 DEmRNA-DEmiRNA interaction pairs including 41 DEmRNAs (26 up-regulated and 15 down-regulated) and 7 down-regulated DEmiRNAs were identified (Figure 3a). chi-miR–200a (degree = 20), chi-miR–141 (degree = 20), chi-miR–182 (degree = 16), chi-miR–206 (degree = 10) and chi-miR–122 (degree = 7) were the top 5 DEmiRNAs that owned most of target DEmRNAs. *BTLA* (degree = 5), *C1orf887* (degree = 4) and *ENSCHIF00000015853* (degree = 4) were the hub genes.For Uni-L vs Mul-L, a total of 153 DEmRNA-DEmiRNA interaction pairs including 56 DEmRNAs (41 up-regulated and 15 down-regulated) and 16 down-regulated DEmiRNAs (4 up-regulated and 12 down-regulated) were identified (Figure 3b). chi-miR–141 (degree = 17), chi-miR–182 (degree = 13), chi-miR–122 (degree = 12), chi-miR–154b–3p (degree = 12) were the top DEmiRNAs that owned most of target DEmRNAs. *CLCA1* (degree = 7), *ENSCHIG00000017462* (degree = 6), *ENSCHIG00000015853* (degree = 5), *SERPINA5* (degree = 5) and *CLEC4G (*degree = 5) were the hub genes.

In order to further narrow the scope of genes and obtain better candidate genes, DEmRNAs were screened according to FPKM >1 of at least three samples per group. Then, 19 pairs and 19 pairs of DEmRNA-DEmiRNAs were obtained from Uni-S vs Mul-S and Uni-L vs Mul-L, respectively (Figure 3c-d). Among them, higher expression of *TNFAIP6* (degree = 3), *CD36* (degree = 3), *BTK* (degree = 2) and *AKAP4* (degree = 2) in Uni-S vs Mul-S, and *ENSCHIG00000017462* (degree = 6), *SERPINA5* (degree = 5) and *PTGFR* (degree = 4) in Uni-L vs Mul-L.

6. Validation by qRT-PCR

Total six DEmRNAs and five DEmiRNAs randomly selected for verification by qRT-PCR. Based on the RNA-sequencing results, *3BHSD* and *STAR* were up-regulated and *LEPR* was down-regulated in Uni-S vs Mul-S. *CCL21, RARRES1* and *DPT* were down-regulated in Uni-L vs Mul-L. The qRT-PCR results were consistent with the RNA-sequencing results generally (Figure 4).

Discussion

Exploring the genetic mechanism of ovulation rate is an important way to improve the kidding rate, which is fundamental to goat production. The greater number of large follicles that stimulate ovulation are believed to be a primary reason for higher ovulation rate [35]. Despite many mRNAs and miRNAs have been found in playing critical roles in ovarian biological processes, the major genes and miRNAs related to ovulation rate and kidding rate have not been identified in goats. In addition, the interaction between mRNAs and miRNAs in follicular development is not yet completely understood. To identify the key genes and miRNAs as well as interactions between them involved in ovulation rate and kidding rate, we

compared DEmRNAs and DEmiRNAs from different sizes of follicles between uniparous and multiple CZ black goats during estrus phase by using RNA-Seq.

The result showed that there were more large follicles in multiple than in uniparous goats (P <0.05), while no difference was observed in small follicles between multiple and uniparous goats, verifying that the higher number of large follicles was related to higher ovulation rate [35]. Based on the RNA sequence data, we identified 119 and 37 DEmRNAs in Uni-S vs Mul-S and Uni-L vs Mul-L, respectively (FPKM >1 of at least three samples per group). These DEmRNAs were involved in the ovarian development related pathways, such as ovarian steroidogenesis, steroid hormone biosynthesis, metabolism of xenobiotics by cytochrome P450 and so on (Figure 2e-f). And many genes (about 37% in Uni-S vs Mul-S and about 41% Uni-L vs Mul-L) had been reported to be associated with reproduction in mammal (data not showed), such as *TNFAIP6, MMP9, INSL3, LEPR, 3BHSD, LHCGR, ARL4C, CD36, CYP11A1, AMDHD1, SPOCK2, AMDHD1, MFAP5, CCL21, PTGFR, SERPINA5,* and so on [19, 41–54]. Of these genes, *TNFAIP6, CYP11A1, CD36, PTGFR* and *SERPINA5* had been reported to be associated with ovulation rate, and *TNFAIP6, CYP11A1* and *CD36* were differentially expressed in Uni-S vs Mul-S, *PTGFR* and *SERPINA5* were in Uni-L vs Mul-L.

TNFAIP6 is a secretory protein of the hyaluronan-binding protein family, which plays a role in cumulus cell stabilisation and expansion, being upregulated in bovine granulosa cells (GCs) during ovulation [41, 55–57]. And *TNFAIP6*-deficient females were sterile in mice[40]. The present study reported that *TNFAIP6* gene expression was 8-fold higher in Mul-S than in Uni-S, suggesting a possible role of *TNFAIP6* gene in the cumulus cells (CCs) expansion in small follicles of multiple goats at estrus phase. *CYP11A1* played a key role in the regulation of steroid-producing pathways in GCs [58]. The first step of steroid biosynthesis pathway was to convert cholesterol into pregnenolone through the action of *CYP11A1* gene in mitochondria, and pregnenolone acted as a substrate for progesterone synthesis through the mediation of *3BHSD* gene [59, 60]. In this study, *CYP11A1* gene was up-regulated in small follicles from multiple goats, which was consistent with the reports in goat ovary [12], demonstrating that *CYP11A1* gene might perform multiple roles in ovarian development in goat. *CD36* is a multifunctional receptor-binding autocrine growth factor that can regulate angiogenesis, cell growth and adhesion. The expression of *CD36* genewas follicle-type dependent with the greatest expression in atretic follicles, and the lowest in healthy follicles[61–64]. Knockdown of *CD36* gene had been shown to increase proliferation and expression of survival and angiogenic in granulosa, endothelial and tumor cells [63]. In this study, *CD36* gene was up-regulated in uniparous goats and participated in hematopoietic cell lineage, speculating that *CD36* gene may affect litter size by affecting the proliferation of GCs or angiogenesis. Overall, *TNFAIP6* and *CYP11A1* genes played a positive role in the regulation of ovulation, while *CD36* gene was contributed to follicular atretic. Accordingly, *TNFAIP6* and *CYP11A1* genes was upregulated in small follicles of multiple goats in our study, and *CD36* gene was downregulated, indicating that there were more small follicles could grow up to dominant follicle in multiple goat. Thus, these genes might play a key role in ovulation rate or kidding rate in goat.

In GCs of periovulatory follicles and corpus luteum (CL) of mice, the expression of *PTGFR* was drastically reduced [65]. For human and primates, *PTGFR* stimulation promotes functional luteolysis only when *PTGFRs* relocated from the cytoplasm to the perinuclear region, which may be a necessary step in the initiation of luteolysis in monkey[66]. Our result showed that *PTGFR* gene was downregulated in large follicles from multiple goats, suggesting that the greater reduction of *PTGFR* gene expression in multiple goats may contribute to ovulate more. The previous studies reported that *SERPINA5,* as a protease inhibitor, was expressed in the reproductive tract of adult mice and in the GCs of bovine follicles, and was highly expressed in bovine healthy follicles [54, 67]. *SERPINA5* gene was down-regulated in ovarian cancer (OC) studies [68–70]. We found that *SERPINA5* gene was up-regulated in large follicles from multiple goats, suggesting that *SERPINA5* gene may affect follicular development and kidding ratein goat. Take it together, the downregulation of *PTGFR* gene and upregulation of *SERPINA5* gene in large follicles would be helpful to ovulate more in multiple goats.

We identified seven and sixteen differentially expressed miRNAs in Uni-S and Mul-S and Uni-L and Mul-L groups, respectively. And miR–200a, miR–451–5p, miR–141, miR–182, miR–206 and miR–122 was highly expressed miRNAs in Uni-S and Mul-S groups, miR–1, miR–206, miR–133a–3p, miR–133b, miR–182, miR–215–5p, miR–122 and miR–451–5p was highly expressed miRNAs in Uni-L and Mul-L groups. However, only miR–200a were reported highly expressed in the ovaries of goats [1], demonstrating that the expression of miRNAs in whole ovary, small follicles and large follicles were independent of each other. Of these 14 highly expressed DEmiRNAs, miR–200a, miR–141, miR–1, miR–206, miR–133b, miR–133a–3p, miR–182 and miR–122 had been reported to play important roles in basic reproductive activities. miR–200a was more abundant in ovarian tissue during the luteal phase and may have an important role in the follicular-luteal transition by binding to *LHR* mRNA directly in sheep [71]. miR–200a was frequently overexpressed and was closely related to the cell migratory, cell proliferation and invasive abilities in ovarian [72–74]. miR–141 was significantly upregulated in OC cell lines and advanced metastatic ovarian cancers [75, 76]., and it might inhibit granulosa cell apoptosis by targeting *DAPK1* through MAPK signaling pathway and further lead to the development of polycystic ovary syndrome [77]. In this study, miR–200a and miR–141 were upregulated in small follicles of uniparous goats, suggesting that they might affect the normal development of granulosa cells, thereby affected maturation of the oocyte, and finally reducing ovulation rate. miR–206 and miR–1 were the potential tumor suppressor and down-regulated in OC tissues, and they both can inhibit *c-Met* expression and regulate cell proliferation, migration and invasion [78, 79]. miR–206 inhibited OC cell proliferation, migration and invasion, and induced apoptosis [78, 80, 81]. miR–206 and miR–1were downregulated in large follicles from multiple goats in our study, which may be related to the maturation of the oocyte and ovulation in goat. miR–133 family (miR–133a–3p and miR–133b) had been involved in regulation of many cellular processes such as cell proliferation, apoptosis, migration and invasion [82, 83]. miR–133a–3p was the target of LncRNA HOXD-AS1, whcih promoted the proliferation, invasion, and EMT process of EOC cells and activated Wnt/β-catenin signaling pathway [84]. *Foxl2* is a conserved, early-acting gene in vertebrate ovarian development, and play an important role on proliferation of GCs and maturation of the oocyte [61, 62]. Recently, the *Foxl2* gene has been reported to be regulated by miR–133b. miR–133b can bind to the

Foxl2–3'UTR in GCs to inhibit the expression of the downstream genes *STAR* and *CYP19A1,* which can promote estrogen secretion in granulosa cells simultaneously [85]. miR–133b was up-regulated more than 30-fold in MI oocytes after IGF–1 treatment, and may play important roles in the growth and maturation of oocytes by regulating its potential target gene *TAGLN2* [86].

Compared with Uni-S vs Mul-S and Uni-L vs Mul-L, miR–182 and miR–122 were differentially expressed in both groups. miR–182 was up-regulated in follicular fluid of polycystic ovary syndrome (PCOS) patients [87], and it's expression was significantly increased in OC cell lines and tissues [88]. miR–122 inhibited epithelial mesenchymal transition by regulating *P4HA1* in OC cells [39]. miR–122 played a regulatory role in *LHCGR* expression, which were crucial for mediating LH action in growing follicles, by modulating LRBP levels during FSH-induced follicle growth [89]. miR–122 mediated *LHR* mRNA levels by modulating the expression of *LRBP* through the regulation of *SREBP* activation, which were crucial for supporting key reproductive processes such as ovulation and CL function [90]. In this study, miR–182 and miR–122 both were upregulated in uniparous goat, suggesting that they may affect ovulation rate by affecting follicular growth in uniparous goats.

Taken together, this study showed that *CD36, TNFAIP6, CYP11A1, SERPINA5* and *PTGFR* would be related to ovarian follicular development and luteinization in goat, but their upstream determinants were still uncertain. By predicting the target genes of DEmiRNAs, high expression of *CD36* (miR–122, miR–200a), *TNFAIP6* (miR–200a, miR–182), *CYP11A1* (miR–122), *SERPINA5* (miR–1, miR–206, miR–133a–3p, miR–133b) and *PTGFR* (miR–182, miR–122) were screened (Figure 6), which may be related to ovulation and kidding rate.

Conclusion

Identifying the precise subset of genes and miRNAs involved during follicle development is essential to fully comprehend the cascade of events leading to ovulation of the follicle, and will likely contribute to a better control of fertility. The study provides the first identification of the DEmRNAs and DEmiRNAs as well as their interactions in the follicles of multiple and uniparous goats at estrus phase by using RNA-seq technology. *CD36* (miR–122, miR–200a), *TNFAIP6* (miR–200a, miR–182), *CYP11A1* (miR–122), *SERPINA5* (miR–1, miR–206, miR–133a–3p, miR–133b) and *PTGFR* (miR–182, miR–122) might play a critical role in goat prolificacy. This study laid a solid foundation for elucidating the regulatory mechanisms of mRNAs and miRNAs in CZ black goat and provides a unique source for exploring miRNA targets in the future.

Materials And Methods

1. Ethics statement

All experiments and sample collections with CZ black goats used in the present study were performed in strict accordance with the Regulation on the Administration of Laboratory Animals (2017 Revision,

CLI.2.293192, State Council, China). The animal experiment protocol was approved by the Institutional Animal Care and Use Committees (IACUCs) of South China Agricultural University (Approval No. 2018-P002). All efforts were made to minimize animal suffering.

2. Animals and sample preparation

In the present study, CZ goats were obtained from the South China Agriculture University, Guangdong, China. A total of eleven healthy female goats with the same age (about 3.5–4.5 years old) and more than three litters were raised under similar conditions of free access to food and water in natural lighting. Six goats were multiple goats with about 2.8 kids per pregnancy, while five goats were uniparous goats with only one kid per pregnancy. Mul: the six goats had three litters which kidding ≥ 2. Uni: the five goats had three litters which kidding = 1.

In order to achieve synchronize estrus, each goat was injected intramuscularly with 0.1 mg chloroprostenol on the same day. Eighteen days later, male goats (vasectomy and ligation of vas deferens) were used to confirm whether the does were estrous. With 24 hours after estrus (in the middle of estrus), all goats were weighed and slaughtered at a local slaughterhouse. The intact ovaries were rapidly collected and washed with PBS thrice. The small follicles (S, diameter (d) <3 mm) or large antral follicles (L, d >1 cm) were isolated from ovarian stromal tissue with tweezers by immersing the ovary in PBS, then placed in liquid nitrogen (Table 5).

3. RNA extraction and qualification

Total RNA was extracted from the whole ovarian follicle by using Trizol reagent (Invitrogen, Carlsbad, CA, USA) according to the manual instruction. The RNA quality was evaluated with the Nanodrop ND–2000 spectrophotometer (Thermo Scientific, Wilmington, DE, USA) and Agilent 2100 Bioanalyzer (Agilent Technologies, Palo Alto, Calif.). RNA integrity was checked by using 1% agarose gel.

4. mRNA sequencing and data processing

A total of 3 μg RNA per sample was used as input material for rRNA removal using the Ribo-Zero Magnetic kit (EpiCentre, Madison, Wisconsin, USA). Then, RNA was fragmented into 200–300 bp by ion interruption. The first cDNA strand was synthesized by 6-base random hexamer primers and reverse transcriptase, and the second cDNA strand was synthesized with dUTP instead of dTTP. The library was constructed and amplified according to the size of the fragments (300–400 bp) by PCR and Agilent 2100 Bionalyzer (Agilent Technologies, CA, USA). The hybrid library was uniformly diluted to 2 nM through mixed proportionally the libraries containing different index sequences and formed a single chain library by TruseqTM RNA sample prep kit (Illumina, San Diego, CA, USA). The libraries were sequenced by paired-end sequencing on the HiSeq 2500 sequencer (Illumina, San Diego, CA, USA).

Raw reads of fastq format were then processed through Illumina 1.8 version. The data of each sample were analyzed and the formula of Q value is $Q_{phred} = -10\log_{10}p$. Then raw reads were filtering by

Cutadapt with its standards include removal of 3 'end joints, removal of parts that have at least 20% base mismatch with known joints 10 bp overlap (agatcggaag), and removal of reads with an average mass fraction less than Q_{20}. After trimming the raw reads, the clean reads were mapped to the goat reference genome (GCF_001704415.1_ARS1) Ensembl V96 by Tophat2. The Mismatch of default reads and reference genomic sequence was within 2, and the mapping ratio is generally higher than 70%.

5. Small RNA library construction, sequencing, and data processing

Following extraction and purification, about 2 μg total RNA per sample was used to construct the small RNA library using TruSeq Small RNA Sample prep Kit (Illumina San Diego CA, USA). All libraries for high throughput sequencing of miRNA were amplified through PCR with adding the sequencing connector and the Index part. Then, the 18–36 nt RNA was purified by 6% Novex TBE PAGE gel (1.0 mm, 10 well) and was qualified by using Agilent 2100 Bioanalyzer. Single-stranded cDNA was performed on Bridge PCR followed by single-end sequencing on an Illumina on the HiSeq 2500 sequencer (Illumina, San Diego, CA, USA).

Raw reads were processed with the script developed by the company consisting of index trimming, read alignment and read counting. The resected clean reads was mapped to the goat reference genome by miRDeep2, in which the mapper.pl program invokes Bowtie, for the alignment between the de-repeat sequence and the reference genome sequence. The de-repeat sequences were aligned to the mature miRNA and precursor miRNA sequences of the species in the miRBase (http://www.mirbase.org/) [91], and the detected miRNA was annotated. Using mireap to analyze unannotated sequences of information, a new miRNA prediction analysis was carried out. According to the number of sequences of miRNA mature bodies of this species, the reads count values of miRNA were calculated.

6. Identifiaction of DEmRNAs and DEmiRNAs

In RNA sequencing analysis, the criteria for measuring mRNA and miRNA expression levels were FPKM (Fragments Per Kilobase of exon model per Million mapped reads) and CPM (CPM = C/N×1000000; C is the Reads number of the gene, and N is the total Reads number of the gene) values, respectively. Differential expression in each group were identified by using DESeq package (version 1.18.0) in R, DEmRNAs and DEmiRNAs were identified with the $|\log_2 \text{FoldChange}|>1$ and P-value<0.05 as the cut-off criteria.

The volcanic diagrams of differentially expressed genes were drawn by R language ggplots2 software package. All genes and samples were clustered by using R language Pheatmap software package. The distance was calculated by Euclidean method according to the expression level of the same gene in different samples and the expression patterns of different genes in the same sample. The longest distance method of hierarchical clustering (Complete Linkage) is used for clustering.

7. Prediction of target gene and construction of mRNA-miRNA interaction network

In this study, miRanDa was used to predict the target genes of DEmiRNA. The target genes of DEmiRNA sequences were predicted by using the 3'UTR sequence of the mRNA of the species as the target sequence. Because of too many target genes, the data were re-filtered and criteria was that the gene could only be retained in FPKM >1 of at least three samples each group. Based on the re-filtered data, DEmRNA-DEmiRNA pairs in Uni-S vs Mul-S and Uni-L vs Mul-L were constructed.

8. Function enrichment analysis

GO (http://geneontology.org/) enrichment and KEGG (http://www.kegg.jp/) pathway analyzed DEmRNAs and target genes of DEmiRNAs. The degree of enrichment was measured by Richfactor, FDR and the number of genes that were enriched into this pathway. Both GO terms and KEGG pathways were corrected. *P*-value ≤ 0.05 was considered to be significantly enriched.

9. RNA preparation and quantitative real-time PCR analysis

Firstly, Total RNA was extracted from ovarian follicles with Total RNA kit (OMEGA, USA) for qRT-PCR of DEmRNA and DEmiRNA. Secondly, the levels of DEmRNAs were measured by the PrimeScript® RT Reagent Kit With gDNA Eraser (TaKaRa, China) and qRT-PCR using SYBR® Green PCR Supermix (Bio-Rad, USA). Each 20 μL reaction included 10 μL of SYBR® Green PCR Supermix, 1 μL of each divergent primer, 1 μL of cDNA and 7 μL of RNase-free water. The cycling conditions included an initial single cycle (95℃ for 1 min), followed by 34 cycles (95℃ for 30s; 58℃ for 30s; 72℃ for 1min). Melting-curve analyses were performed to verify the product identity. Then, the levels of DEmiRNAs were measured by qRT-PCR using miDETECT A Track TM miRNA qRT-PCR Starter kit (RiboBio, Guangzhou, China). Each 20 μL reaction included 10 μL of SYBR Green Mix, 0.5 μL of each divergent primer, 1 μL of cDNA and 8 μL of RNase-free water. The cycling conditions included an initial single cycle (95℃ for 10 min), followed by 40 cycles (95℃ for 5s; 60℃ for 30s; 72℃ for 30s). Melting-curve analyses were performed to verify the product identity.

According to the results of RNA-Seq, 6 DEmRNAs and 5 DEmiRNAs were selected for validation by using qRT-PCR. Primers for DEmRNAs and DEmiRNAs were obtained from Sangon Biotech (Shanghai, China) and RiboBio Company (Guangzhou, China), respectively. The information of the quantitative primers used in this experiment is listed in Table 6. *Actin-β* and *U6* were used as endogenous controls for mRNA and miRNA, respectively, and all reactions were performed in triplicate. Relative expression levels were analyzed via the $2^{-\Delta\Delta Ct}$ method. The changes of gene expression levels between qRT-PCR results and RNA-seq results were calculated and compared.

Abbreviations

miRNAs: microRNAs; CZ black goat: Chuanzhong black goat; FPKM: Fragments Per Kilobase of exon model per Million mapped reads; GO: Gene ontology; KEGG: Kyoto encyclopedia of genes and genomes; RNA-seq: RNA sequencing; qRT-PCR: Quantitative real time polymerase chain reaction; DEmiRNA:

Different expressed miRNA; DEmRNA: Different expressed mRNA; GH: Growth hormone; GCs: Granulosa cells; CCs: Cumulus cells; CL: Corpus luteum; OC: Ovarian cancer; PCOS: Polycystic ovary syndrome

Declarations

Competing interest

The authors declare that they have no competing interests.

Acknowledgements

This research was supported by the Guangdong Provincial Department of Education Youth Innovative Talents Project (2017KQNCX014), the Guangdong Public Welfare Research and Capacity Building Project (2017B020201014, 2017A020208050) and the Guangdong Special plan young top-notch talent (2015TQ01N843).

References

1. Zi XD, Lu JY, Ma L. Identification and comparative analysis of the ovarian microRNAs of prolific and non-prolific goats during the follicular phase using high-throughput sequencing. Sci Rep. 2017; 7(1): 1921.
2. Zi XD, Mu XK, Wang Y. Variation in sequences and mRNA expression levels of growth hormone (GH), insulin-like growth factor I (IGF-I) and II (IGF-II) genes between prolific Lezhi black goat and non-prolific Tibetan goat (Capra hircus). Gen Comp Endocrinol. 2013; 187: 1–5.
3. Cui HX, Zhao SM, Cheng ML, Guo L, Ye RQ, Liu WQ, Gao SZ. Cloning and expression levels of genes relating to the ovulation rate of the Yunling black goat. Biol Reprod. 2009; 80(2): 219–226.
4. Liu Y, Qi B, Xie J, Wu X, Ling Y, Cao X, Kong F, Xin J, Jiang X, Wu Q, Wang W, Li Q, Zhang S, Wu F, Zhang D, Wang R, Zhang X, Li W. Filtered reproductive long non-coding RNAs by genome-wide analyses of goat ovary at different estrus periods. BMC Genomics. 2018; 19(1): 866.
5. Zhang J, Xu Y, Liu H, Pan Z. MicroRNAs in ovarian follicular atresia and granulosa cell apoptosis. Reprod Biol Endocrinol. 2019; 17(1): 9.
6. Gougeon A. Regulation of ovarian follicular development in primates: facts and hypotheses. Endocr Rev. 1996; 17(2): 121–155.
7. Wang X, Zou P, He Y, Meng K, Quan F, Zhang Y. Effect of luteinizing hormone on goat theca cell apoptosis and steroidogenesis through activation of the PI3K/AKT pathway. Anim Reprod Sci. 2018; 190: 108–118.
8. Zhang GM, Deng MT, Lei ZH, Wan YJ, Nie HT, Wang ZY, Fan YX, Wang F, Zhang YL. Effects of NRF1 on steroidogenesis and apoptosis in goat luteinized granulosa cells. Reproduction. 2017; 154(2): 111–122.

9. Han P, Xin H, Peng J, Hou J, Zhang L, Song Y, Li G, Cao B, An X. Identification and expression of X-linked inhibitor of apoptosis protein during follicular development in goat ovary. Theriogenology. 2017; 98: 30–35.
10. Yang D, Jiang T, Lin P, Chen H, Wang L, Wang N, Zhao F, Wang A, Jin Y. Knock-down of apoptosis inducing factor gene protects endoplasmic reticulum stress-mediated goat granulosa cell apoptosis. Theriogenology. 2017; 88: 89–97.
11. Yang D, Wang L, Lin P, Jiang T, Wang N, Zhao F, Chen H, Tang K, Zhou D, Wang A, Jin Y. An immortalized steroidogenic goat granulosa cell line as a model system to study the effect of the endoplasmic reticulum (ER)-stress response on steroidogenesis. J Reprod Dev. 2017; 63(1): 27–36.
12. Wong QW, Sun MA, Lau SW, Parsania C, Zhou S, Zhong S, Ge W. Identification and characterization of a specific 13-miRNA expression signature during follicle activation in the zebrafish ovary. Biol Reprod. 2018; 98(1): 42–53.
13. Yang Y, Lin P, Chen F, Wang A, Lan X, Song Y, Jin Y. Luman recruiting factor regulates endoplasmic reticulum stress in mouse ovarian granulosa cell apoptosis. Theriogenology. 2013; 79(4): 633–639.
14. Zhang Y, Yan Z, Qin Q, Nisenblat V, Chang HM, Yu Y, Wang T, Lu C, Yang M, Yang S, Yao Y, Zhu X, Xia X, Dang Y, Ren Y, Yuan P, Li R, Liu P, Guo H, Han J, He H, Zhang K, Wang Y, Wu Y, Li M, Qiao J, Yan J, Yan L. Transcriptome landscape of human folliculogenesis reveals oocyte and granulosa cell interactions. Mol Cell. 2018; 72(6): 1021–1034.
15. Zhang J, Liu Y, Yao W, Li Q, Liu H, Pan Z. Initiation of follicular atresia: gene networks during early atresia in pig ovaries. Reproduction. 2018; 156(1): 23–33.
16. Hatzirodos N, Irving-Rodgers HF, Hummitzsch K, Harland ML, Morris SE, Rodgers RJ. Transcriptome profiling of granulosa cells of bovine ovarian follicles during growth from small to large antral sizes. BMC Genomics. 2014; 15: 24.
17. Di Pietro M, Scotti L, Irusta G, Tesone M, Parborell F, Abramovich D. Local administration of platelet-derived growth factor B (PDGFB) improves follicular development and ovarian angiogenesis in a rat model of Polycystic Ovary Syndrome. Mol Cell Endocrinol. 2016; 433: 47–55.
18. Huang Y, Yao XL, Meng JZ, Liu Y, Jiang XL, Chen JW, Li PF, Ren YS, Liu WZ, Yao JB, Folger JK, Smith GW, Lv LH. Intrafollicular expression and potential regulatory role of cocaine- and amphetamine-regulated transcript in the ovine ovary. Domest Anim Endocrinol. 2016; 54: 30–36.
19. Zi XD, Lu JY, Zhou H, Ma L, Xia W, Xiong XR, Lan DL, Wu XH. Comparative analysis of ovarian transcriptomes between prolific and non-prolific goat breeds via high-throughput sequencing. Reprod Domest Anim. 2018; 53(2): 344–351.
20. Ling Y, Xu L, Zhu L, Sui M, Zheng Q, Li W, Liu Y, Fang F, Zhang X. Identification and analysis of differentially expressed long non-coding RNAs between multiparous and uniparous goat (Capra hircus) ovaries. PLoS One. 2017; 12(9): e183163.
21. Lai FN, Zhai HL, Cheng M, Ma JY, Cheng SF, Ge W, Zhang GL, Wang JJ, Zhang RQ, Wang X, Min LJ, Song JZ, Shen W. Whole-genome scanning for the litter size trait associated genes and SNPs under selection in dairy goat (Capra hircus). Sci Rep. 2016; 6: 38096.

22. An XP, Hou JX, Zhao HB, Li G, Bai L, Peng JY, M YQ, Song YX, Wang JG, Cao BY. Polymorphism identification in goat GNRH1 and GDF9 genes and their association analysis with litter size. Anim Genet. 2013; 44(2): 234–238.
23. Zi XD, Xu HW, Wang Y. Variation in sequences and mRNA expression levels of inhibin subunits alpha (INHA) and betaA (INHBA) genes between prolific and nonprolific goat breeds. Mol Reprod Dev. 2012; 79(4): 238.
24. Yang CX, Zi XD, Wang Y, Yang DQ, Ma L, Lu JY, Niu HR, Xiao X. Cloning and mRNA expression levels of GDF9, BMP15, and BMPR1B genes in prolific and non-prolific goat breeds. Mol Reprod Dev. 2012; 79(1): 2.
25. Ling YH, Ren CH, Guo XF, Xu LN, Huang YF, Luo JC, Zhang YH, Zhang XR, Zhang ZJ. Identification and characterization of microRNAs in the ovaries of multiple and uniparous goats (Capra hircus) during follicular phase. BMC Genomics. 2014; 15: 339.
26. Yang W, Yan H, Wang K, Cui Y, Zhou T, Xu H, Zhu H, Liu J, Lan X, Qu L, Pan C, Zhang E. Goat PDGFRB: unique mRNA expression profile in gonad and significant association between genetic variation and litter size. R Soc Open Sci. 2019; 6(1): 180805.
27. Kang Z, Jiang E, Wang K, Pan C, Chen H, Yan H, Zhu H, Liu J, Qu L, Lan X. Goat membrane associated ring-CH-type finger 1 (MARCH1) mRNA expression and association with litter size. Theriogenology. 2019; 128: 8–16.
28. Cui Y, Yan H, Wang K, Xu H, Zhang X, Zhu H, Liu J, Qu L, Lan X, Pan C. Insertion/deletion within the KDM6A gene is significantly associated with litter size in goat. Front Genet. 2018; 9: 91.
29. Wang K, Yan H, Xu H, Yang Q, Zhang S, Pan C, Chen H, Zhu H, Liu J, Qu L, Lan X. A novel indel within goat casein alpha S1 gene is significantly associated with litter size. Gene. 2018; 671: 161–169.
30. Silpa MV, Naicy T, Aravindakshan TV, Radhika G, Boswell A, Mini M. Sirtuin3 (SIRT3) gene molecular characterization and SNP detection in prolific and low prolific goat breeds. Theriogenology. 2018; 122: 47–52.
31. An XP, Hou JX, Li G, Song YX, Wang JG, Chen QJ, Cui YH, Wang YF, Cao BY. Polymorphism identification in the goat KITLG gene and association analysis with litter size. Anim Genet. 2012; 43(1): 104–107.
32. Yang Q, Yan H, Li J, Xu H, Wang K, Zhu H, Chen H, Qu L, Lan X. A novel 14-bp duplicated deletion within goat GHR gene is significantly associated with growth traits and litter size. Anim Genet. 2017; 48(4): 499–500.
33. Wang K, Hui Y, Zhang S, Wang M, Yan H, Zhu H, Qu L, Lan X, Pan C. A deletion mutation within the ATBF1 gene is strongly associated with goat litter size. Anim Biotechnol. 2019: 1–7.
34. Hou J, An X, Li G, Wang Y, Song Y, Cao B. Exploring polymorphisms and their effects on reproductive traits of the INHA and INHbetaA genes in three goat breeds. Anim Sci J. 2012; 83(4): 273–278.
35. Pramod RK, Sharma SK, Singhi A, Pan S, Mitra A. Differential ovarian morphometry and follicular expression of BMP15, GDF9 and BMPR1B influence the prolificacy in goat. Reprod Domest Anim. 2013; 48(5): 803–809.

36. Zhang C, Liu Y, Huang K, Zeng W, Xu D, Wen Q, Yang L. The association of two single nucleotide polymorphisms (SNPs) in growth hormone (GH) gene with litter size and superovulation response in goat-breeds. Genet Mol Biol. 2011; 34(1): 49–55.
37. Ling YH, Quan Q, Xiang H, Zhu L, Chu MX, Zhang XR, Han CY. Expression profiles of differentially expressed genes affecting fecundity in goat ovarian tissues. Genet Mol Res. 2015; 14(4): 18743–18752.
38. An X, Song Y, Hou J, Li G, Zhao H, Wang J, Cao B. Identification and profiling of microRNAs in the ovaries of polytocous and monotocous goats during estrus. Theriogenology. 2016; 85(4): 769–780.
39. Li L, Zhang J, Zhu JQ, Gu S, Sun Q, Zhou GM, Fu CX, Li Q, Chen LY, Li DX, Liu SJ, Yang ZR. Genetic diversity of nine populations of the black goat (Capra hircus) in Sichuan, PR China. Zoolog Sci. 2006; 23(3): 229–234.
40. Yu J. Genetic Diversity of mtDNA D-loop of different black goat breeds in Sichuan Province. Journal of Anhui Agricultural Sciences. 2010.
41. Lussier JG, Diouf MN, Levesque V, Sirois J, Ndiaye K. Gene expression profiling of upregulated mRNAs in granulosa cells of bovine ovulatory follicles following stimulation with hCG. Reprod Biol Endocrinol. 2017; 15(1): 88.
42. Kfir S, Basavaraja R, Wigoda N, Ben-Dor S, Orr I, Meidan R. Genomic profiling of bovine corpus luteum maturation. PLoS One, 2018. 13(3): p. e0194456.
43. Pelusi C, Fanelli F, Pariali M, Zanotti L, Gambineri A, Pasquali R. Parallel variations of insulin-like peptide 3 (INSL3) and antimullerian hormone (AMH) in women with the polycystic ovary syndrome according to menstrual cycle pattern. J Clin Endocrinol Metab, 2013. 98(10): p. E1575–82.
44. Batista AM, Silva DM, Rego MJ, Silva FL, Silva EC, Beltrao EI, Gomes Filho MA, Wischral A, Guerra MM. The expression and localization of leptin and its receptor in goat ovarian follicles. Anim Reprod Sci, 2013. 141(3–4): p. 142–7.
45. Convissar S, Winston NJ, Fierro MA, Scoccia H, Zamah AM, Stocco C. Sp1 regulates steroidogenic genes and LHCGR expression in primary human luteinized granulosa cells. J Steroid Biochem Mol Biol, 2019. 190: p. 183–192.
46. Wakinoue S, Chano T, Amano T, Isono T, Kimura F, Kushima R, Murakami T. ADP-ribosylation factor-like 4C predicts worse prognosis in endometriosis-associated ovarian cancers. Cancer Biomark, 2019. 24(2): p. 223–229.
47. Zhang N, Wang L, Luo G, Tang X, Ma L, Zheng Y, Liu S, A Price C, Jiang Z. Arachidonic acid regulation of intracellular signaling pathways and target gene expression in bovine ovarian granulosa cells. Animals (Basel), 2019. 9(6).
48. Dentis JL, Schreiber NB, Burress AM, Spicer LJ. Effects of angiogenin on granulosa and theca cell function in cattle. Animal, 2017. 11(5): p. 811–819.
49. Angulo L, Guyader-Joly C, Auclair S, Hennequet-Antier C, Papillier P, Boussaha M, Fritz S, Hugot K, Moreews F, Ponsart C, Humblot P, Dalbies-Tran R. An integrated approach to bovine oocyte quality: from phenotype to genes. Reprod Fertil Dev, 2015.

50. Ren F, Wang D, Wang Y, Chen P, Guo C. SPOCK2 affects the biological behavior of endometrial cancer cells by regulation of MT1-MMP and MMP2. Reprod Sci, 2019: p. 1933719119834341.
51. Leung CS, Yeung TL, Yip KP, Pradeep S, Balasubramanian L, Liu J, Wong KK, Mangala LS, Armaiz-Pena GN, Lopez-Berestein G, Sood AK, Birrer MJ, Mok SC. Calcium-dependent FAK/CREB/TNNC1 signalling mediates the effect of stromal MFAP5 on ovarian cancer metastatic potential. Nat Commun, 2014. 5: p. 5092.
52. Ignacio RMC, Lee ES, Wilson AJ, Beeghly-Fadiel A, Whalen MM, Son DS. Chemokine network and overall survival in TP53 wild-type and mutant ovarian cancer. Immune Netw, 2018. 18(4): p. e29.
53. Chang J, Frandsen S, D'Annibale-Tolhurst M, Palumbo N, Gadsby J. Prostaglandin (PTG) E and F receptors in the porcine corpus luteum; effect of tumor necrosis factor-alpha. Anim Reprod Sci, 2018. 195: p. 139–148.
54. Hayashi KG, Ushizawa K, Hosoe M, Takahashi T. Differential gene expression of serine protease inhibitors in bovine ovarian follicle: possible involvement in follicular growth and atresia. Reprod Biol Endocrinol, 2011. 9: p. 72.
55. Sayasith K, Bouchard N, Dore M, Sirois J. Regulation of bovine tumor necrosis factor-alpha-induced protein 6 in ovarian follicles during the ovulatory process and promoter activation in granulosa cells. Endocrinology. 2008; 149(12): 6213–6225.
56. Fulop C, Szanto S, Mukhopadhyay D, Bardos T, Kamath RV, Rugg MS, Day AJ, Salustri A, Hascall VC, Glant TT, Mikecz K. Impaired cumulus mucification and female sterility in tumor necrosis factor-induced protein–6 deficient mice. Development. 2003; 130(10): 2253–2261.
57. Assidi M, Dufort I, Ali A, Hamel M, Algriany O, Dielemann S, Sirard MA. Identification of potential markers of oocyte competence expressed in bovine cumulus cells matured with follicle-stimulating hormone and/or phorbol myristate acetate in vitro. Biol Reprod. 2008; 79(2): 209–222.
58. Bakhshalizadeh S, Amidi F, Shirazi R, Shabani Nashtaei M. Vitamin D3 regulates steroidogenesis in granulosa cells through AMP-activated protein kinase (AMPK) activation in a mouse model of polycystic ovary syndrome. Cell Biochem Funct, 2018. 36(4): p. 183–193.
59. Manna PR, Stetson CL, Slominski AT, Pruitt K. Role of the steroidogenic acute regulatory protein in health and disease. Endocrine, 2016. 51(1): p. 7–21.
60. Liang D, Fan Z, Zou Y, Tan X, Wu Z, Jiao S, Li J, Zhang P, You F. Characteristics of Cyp11a during gonad differentiation of the Olive Flounder Paralichthys olivaceus. Int J Mol Sci, 2018. 19(9).
61. Bertho S, Herpin A, Branthonne A, Jouanno E, Yano A, Nicol B, Muller T, Pannetier M, Pailhoux E, Miwa M, Yoshizaki G, Schartl M, Guiguen Y. The unusual rainbow trout sex determination gene hijacked the canonical vertebrate gonadal differentiation pathway. Proc Natl Acad Sci U S A. 2018; 115(50): 12781–12786.
62. Loffler KA, Zarkower D, Koopman P. Etiology of ovarian failure in blepharophimosis ptosis epicanthus inversus syndrome: FOXL2 is a conserved, early-acting gene in vertebrate ovarian development. Endocrinology. 2003; 144(7): 3237–3243.

63. Osz K, Ross M, Petrik J. The thrombospondin–1 receptor CD36 is an important mediator of ovarian angiogenesis and folliculogenesis. Reprod Biol Endocrinol, 2014. 12: p. 21.
64. Serke H, Bausenwein J, Hirrlinger J, Nowicki M, Vilser C, Jogschies P, Hmeidan FA, Blumenauer V, Spanel-Borowski K. Granulosa cell subtypes vary in response to oxidized low-density lipoprotein as regards specific lipoprotein receptors and antioxidant enzyme activity. J Clin Endocrinol Metab, 2010. 95(7): p. 3480–90.
65. Lee-Thacker S, Choi Y, Taniuchi I, Takarada T, Yoneda Y, Ko C, Jo M. Core binding factor beta expression in ovarian granulosa cells is essential for female fertility. Endocrinology, 2018. 159(5): p. 2094–2109.
66. Kim SO, Markosyan N, Pepe GJ, Duffy DM. Estrogen promotes luteolysis by redistributing prostaglandin F2alpha receptors within primate luteal cells. Reproduction, 2015. 149(5): p. 453–64.
67. Zhang X, Huang L, Wu T, Feng Y, Ding Y, Ye P, Yin Z. Transcriptomic analysis of ovaries from pigs with high and low litter size. PLoS One, 2015. 10(10): p. e0139514.
68. Yang H, Geiger M. Cell penetrating SERPINA5 (ProteinC inhibitor, PCI): More questions than answers. Semin Cell Dev Biol, 2017. 62: p. 187–193.
69. Jing Y, Jia D, Wong CM, Oi-Lin Ngl, Zhang Z, Liu L, Wang Q, Zhao F, Li J, Yao M, Wu X, He X. SERPINA5 inhibits tumor cell migration by modulating the fibronectin-integrin beta1 signaling pathway in hepatocellular carcinoma. Mol Oncol, 2014. 8(2): p. 366–77.
70. Bijsmans IT, Smits KM, de Graeff P, Wisman GB, van der Zee AG, Slangen BF, de Bruine AP, van Engeland M, Sieben NL, Van de Vijver KK. Loss of SerpinA5 protein expression is associated with advanced-stage serous ovarian tumors. Mod Pathol, 2011. 24(3): p. 463–70.
71. Wang H, Li X, Zhou R, Xi J, Wei Y, Li L, Zhang Z. Genome -wide transcriptome profiling in ovaries of small-tail Han sheep during the follicular and luteal phases of the oestrous cycle. Anim Reprod Sci, 2018. 197: p. 212–221.
72. Suo HB, Zhang KC, Zhao J. MiR–200a promotes cell invasion and migration of ovarian carcinoma by targeting PTEN. Eur Rev Med Pharmacol Sci, 2018. 22(13): p. 4080–4089.
73. Zavesky L, Jandakova E, Weinberger V, Minar L, Hanzikova V, Duskova D, Drabkova LZ, Svobodova I, Horinek A. Ascites-derived extracellular microRNAs as potential biomarkers for ovarian cancer. Reprod Sci, 2019. 26(4): p. 510–522.
74. Wang Y, Qiu C, Lu N, Liu Z, Jin C, Sun C, Bu H, Yu H, Dongol S, Kong B. FOXD1 is targeted by miR–30a–5p and miR–200a–5p and suppresses the proliferation of human ovarian carcinoma cells by promoting p21 expression in a p53-independent manner. Int J Oncol, 2018. 52(6): p. 2130–2142.
75. Zhang M, Ren C, Xiao Y, Xia X, Fang X. Expression profile analysis of circular RNAs in ovarian endometriosis by microarray and bioinformatics. Med Sci Monit, 2018. 24: p. 9240–9250.
76. Mak CS, Yung MM, Hui LM, Leung LL, Liang R, Chen K, Liu SS, Qin Y, Leung TH, Lee KF, Chan KK, Ngan HY, Chan DW. MicroRNA–141 enhances anoikis resistance in metastatic progression of ovarian cancer through targeting KLF12/Sp1/survivin axis. Mol Cancer, 2017. 16(1): p. 11.

77. Li D, Xu D, Xu Y, Chen L, Li C, Dai X, Zhang L, Zheng L. MicroRNA–141–3p targets DAPK1 and inhibits apoptosis in rat ovarian granulosa cells. Cell Biochem Funct, 2017. 35(4): p. 197–201.
78. Dai C, Xie Y, Zhuang X, Yuan Z. MiR–206 inhibits epithelial ovarian cancer cells growth and invasion via blocking c-Met/AKT/mTOR signaling pathway. Biomed Pharmacother, 2018. 104: p. 763–770.
79. Qu W, Chen X, Wang J, Lv J, Yan D. MicroRNA–1 inhibits ovarian cancer cell proliferation and migration through c-Met pathway. Clin Chim Acta, 2017. 473: p. 237–244.
80. Ling C, Liu S, Wang Y, Zhang FC, DU Y. Role of miR–206/CDK4 in modulating the growth and chemotlerapy sensitivity of ovarian cancer cells. Nan Fang Yi Ke Da Xue Xue Bao, 2017. 37(3): p. 393–397.
81. Sheng N, Xu YZ, Xi QH, Jiang HY, Wang CY, Zhang Y, Ye Q. Overexpression of KIF2A is suppressed by miR–206 and associated with poor prognosis in ovarian cancer. Cell Physiol Biochem, 2018. 50(3): p. 810–822.
82. Liu X, Li G. MicroRNA–133b inhibits proliferation and invasion of ovarian cancer cells through Akt and Erk1/2 inactivation by targeting epidermal growth factor receptor. Int J Clin Exp Pathol, 2015. 8(9): p. 10605–14.
83. Hao L, Li J, Tian Y, Wu J. Changes in the microRNA profile of the mandible of ovariectomized mice. Cell Physiol Biochem, 2016. 38(4): p. 1267–87.
84. Zhang Y, Dun Y, Zhou S, Huang XH. LncRNA HOXD-AS1 promotes epithelial ovarian cancer cells proliferation and invasion by targeting miR–133a–3p and activating Wnt/beta-catenin signaling pathway. Biomed Pharmacother, 2017. 96: p. 1216–1221.
85. Dai A, Sun H, Fang T, Zhang Q, Wu S, Jiang Y, Ding L, Yan G, Hu Y. MicroRNA–133b stimulates ovarian estradiol synthesis by targeting Foxl2. FEBS Lett, 2013. 587(15): p. 2474–82.
86. Xiao G, Xia C, Yang J, Liu J, Du H, Kang X, Lin Y, Guan R, Yan P, Tang S. MiR–133b regulates the expression of the Actin protein TAGLN2 during oocyte growth and maturation: a potential target for infertility therapy. PLoS One, 2014. 9(6): p. e100751.
87. Naji M, Nekoonam S, Aleyasin A, Arefian E, Mahdian R, Azizi E, Shabani Nashtaei M, Amidi F. Expression of miR–15a, miR–145, and miR–182 in granulosa-lutein cells, follicular fluid, and serum of women with polycystic ovary syndrome (PCOS). Arch Gynecol Obstet, 2018. 297(1): p. 221–231.
88. Wang A, Jin C, Li H, Qin Q, Li L. LncRNA ADAMTS9-AS2 regulates ovarian cancer progression by targeting miR–182–5p/FOXF2 signaling pathway. Int J Biol Macromol, 2018. 120(Pt B): p. 1705–1713.
89. Duan Y, Dong Y, Dang R, Hu Z, Yang Y, Hu Y, Cheng J. MiR–122 inhibits epithelial mesenchymal transition by regulating P4HA1 in ovarian cancer cells. Cell Biol Int, 2018. 42(11): p. 1564–1574.
90. Menon B, Gulappa T, Menon KM. Molecular regulation of LHCGR expression by miR–122 during follicle growth in the rat ovary. Mol Cell Endocrinol, 2017. 442: p. 81–89.
91. Griffiths-Jones S. The microRNA Registry. Nucleic Acids Res. 2004; 32(Database issue): D109-D111.

Tables

Table 1 Comparison of follicles between Uniparous and Multiple CZ black goat

Groups	The number of follicles		
	Small follicles (d<3 mm)	Large follicles (d>1 cm)	Total number
Uniparous	30.29±4.36 [a]	2.71±0.36 [b]	39.57±3.41 [b]
Multiple	45.83±7.01 [a]	4.83±0.7 [a]	69.17±7.13 [a]

Values are expressed as the means ± standard error.

Different letters denote values within a row, with non-matching superscript letters representing significant differences ($P < 0.05$).

Table 2 Counts of clean reads and mapped ratio of sequencing results

sample	Q30 (%)	Clean Reads (%)	Total Mapped (%)	Uniquely Mapped (%)
1L	94.23	104768836 (99.62)	93091299 (88.85)	89904506 (96.58)
1S	94.26	103870160 (99.62)	89325162 (86.00)	86178560 (96.48)
2L	94.85	100396168 (99.70)	89929580 (89.57)	87064232 (96.81)
2S	94.88	102014414 (99.69)	88224659 (84.48)	85375813 (96.77)
3L	94.15	104879676 (99.48)	96174993 (91.70)	93014775 (96.71)
3S	94.24	102993890 (99.45)	93439661 (90.72)	90706789 (97.08)
4L	92.66	105470926 (99.40)	94602673 (89.70)	90695153 (95.87)
4S	92.27	103362624 (99.45)	89016110 (86.12)	86176140 (96.81)
5L	92.57	102209432 (99.37)	91648613 (89.67)	88135894 (96.17)
5S	94.11	106653668 (99.77)	94898026 (88.98)	91876107 (96.82)
6L	93.86	100346902 (99.75)	90637403 (90.32)	87309742 (96.44)
6S	91.52	105756846 (99.19)	88562076 (83.74)	85171985 (96.17)
7L	92.26	101449700 (99.50)	87567963 (86.32)	84396898 (96.38)
7S	93.79	103645956 (99.58)	91547208 (88.33)	89350437 (97.60)
8L	91.91	102150920 (99.54)	88542997 (86.68)	85076770 (96.09)
8S	92.38	106529902 (99.45)	89051464 (83.59)	85509801 (96.02)
9S	91.87	105002632 (99.51)	90469465 (86.16)	87006833 (96.17)

L (large follicles), S (small follicles)

Table 3 The top 10 DEmRNAs and DEmiRNAs in Uni-S vs Mul-S (a) and Uni-L vs Mul-L (b)

	DEmiRNA	log2fold change	*P*-val	DEmRNA	log2fold change	*P*-val
a	chi-miR-200a	-7.77	3.18E-02	*S100A12*	-3.75	5.93E-05
	chi-miR-141	-7.94	1.18E-02	*MMP9*	-2.55	3.15E-06
	chi-miR-451-5p	-9.01	9.45E-03	*INSL3*	2.39	8.34E-05
	chi-miR-182	-10.62	1.39E-02	*WNT5B*	-1.65	2.25E-06
	chi-miR-184	-11.45	3.83E-02	*ARL4C*	-1.59	7.98E-07
	chi-miR-206	-11.91	1.07E-02	*TGFBI*	-1.55	1.64E-05
	chi-miR-122	-12.44	1.24E-03	*LFNG*	-1.35	8.70E-05
				MAP7D2	1.32	8.68E-05
				SDC1	-1.14	9.74E-05
				NT5E	1.03	1.16E-04
b	chi-miR-496-5p	4.43	2.06E-02	*DPT*	-1.81	8.07E-04
	chi-miR-141	-6.46	5.90E-03	*COL6A6*	1.77	6.14E-03
	chi-miR-1	-7.02	1.25E-02	*MFAP5*	-1.67	6.36E-03
	chi-miR-451-5p	-7.05	6.81E-03	*BRINP3*	-1.52	3.59E-04
	chi-miR-34c-5p	-7.86	2.22E-02	*SPOCK2*	-1.37	1.09E-03
	chi-miR-133b	-9.62	3.12E-03	*RNASE6*	-1.33	7.43E-03
	chi-miR-34b-5p	-9.82	6.78E-03	*XG*	-1.22	5.27E-03
	chi-miR-122	-10.73	2.17E-03	*AMDHD1*	1.19	3.19E-03
	chi-miR-182	-10.83	1.61E-03	*ADAM33*	-1.04	1.01E-02
	chi-miR-206	-12.91	5.17E-03	*CCL21*	-1.01	9.18E-03

Table 4 Top 5 GO term of DEmRNAs in Uni-S vs Mul-S and Uni-L vs Mul-L

Category	Term	DEG	*P*	Term	DEG	*P*
	Uni-S vs Mul-S			Uni-L vs Mul-L		
Biological process	immune system process	45	3.10E-07	anterior/posterior pattern specification	11	1.20E-07
	immune response	24	6.90E-05	definitive hemopoiesis	4	9.30E-06
	steroid biosynthetic process	7	1.20E-04	regionalization	11	1.10E-05
	organic hydroxy compound biosynthetic process	8	2.40E-04	pattern specification process	12	1.10E-05
	superoxide anion generation	4	3.00E-04	skeletal system morphogenesis	9	1.80E-05
Cellular component	cell surface	18	4.40E-05	extracellular region part	13	4.60E-04
	extracellular region	24	7.00E-05	extracellular region	14	5.70E-04
	extracellular space	18	1.20E-04	extracellular matrix	5	2.38E-03
	extracellular region part	21	1.70E-04	cell periphery	25	6.60E-03
	plasma membrane	45	1.08E-03	protein C inhibitor-TMPRSS7 complex	1	6.88E-03
Molecular function	deaminase activity	3	4.90E-04	icosanoid receptor activity	2	1.20E-03
	receptor activity	17	6.30E-04	chloride channel activity	3	2.70E-03
	hydrolase activity, acting on carbon-nitrogen (but not peptide) bonds, in cyclic amidines	3	6.40E-04	drug binding	3	4.20E-03
	glycogen binding	2	6.50E-	chloride	3	4.20E-

			04	transmembrane transporter activity		03
	receptor binding	24	6.70E-04	anion channel activity	3	4.80E-03

DEG, the number of different expressed genes. *P*, *P*-value.

Table 5 Sample characteristics

Index	Number (n)	Age (years old)	S (d<3mm) /per one[1]	L (d>1cm) /per one[2]
Multiple (Mul)	6	3.5-4.5	8-10	1-2
Uniparous (Uni)	5	3.5-4.5	8-10	1-2

[1] Eight to ten small follicles were collected and pooled from each goat.

[2] One to two large follicles were collected from each goat.

Table 6 Primers of DEmRNAs

Gene name	Forward primer (5'-3')	Reverse primer (5'-3')	Product length/bp
3BHSD	agggcatctcagtggtca	ggataaagactggcacgcta	144
LEPR	ccattgagaagtatcagttcagtc	catgctggtgtttttcatcatcttg	105
STAR	cagaagggtgtcatcagagc	tgagcagccaggtgagttt	97
CCL21	ccgaaagaagattcccgcca	ggcgagaacaggatagctgg	90
RARRES1	gcgcgtgggttaatcagaag	acattaacagctggtctgggtt	148
DPT	gtaccagacatgctccaacaa	ctgttgtcagccagcaggaa	137
Actin-β	tgcttctaggcggactgatt	tacaatcaaagtcctcggccac	106

Figures

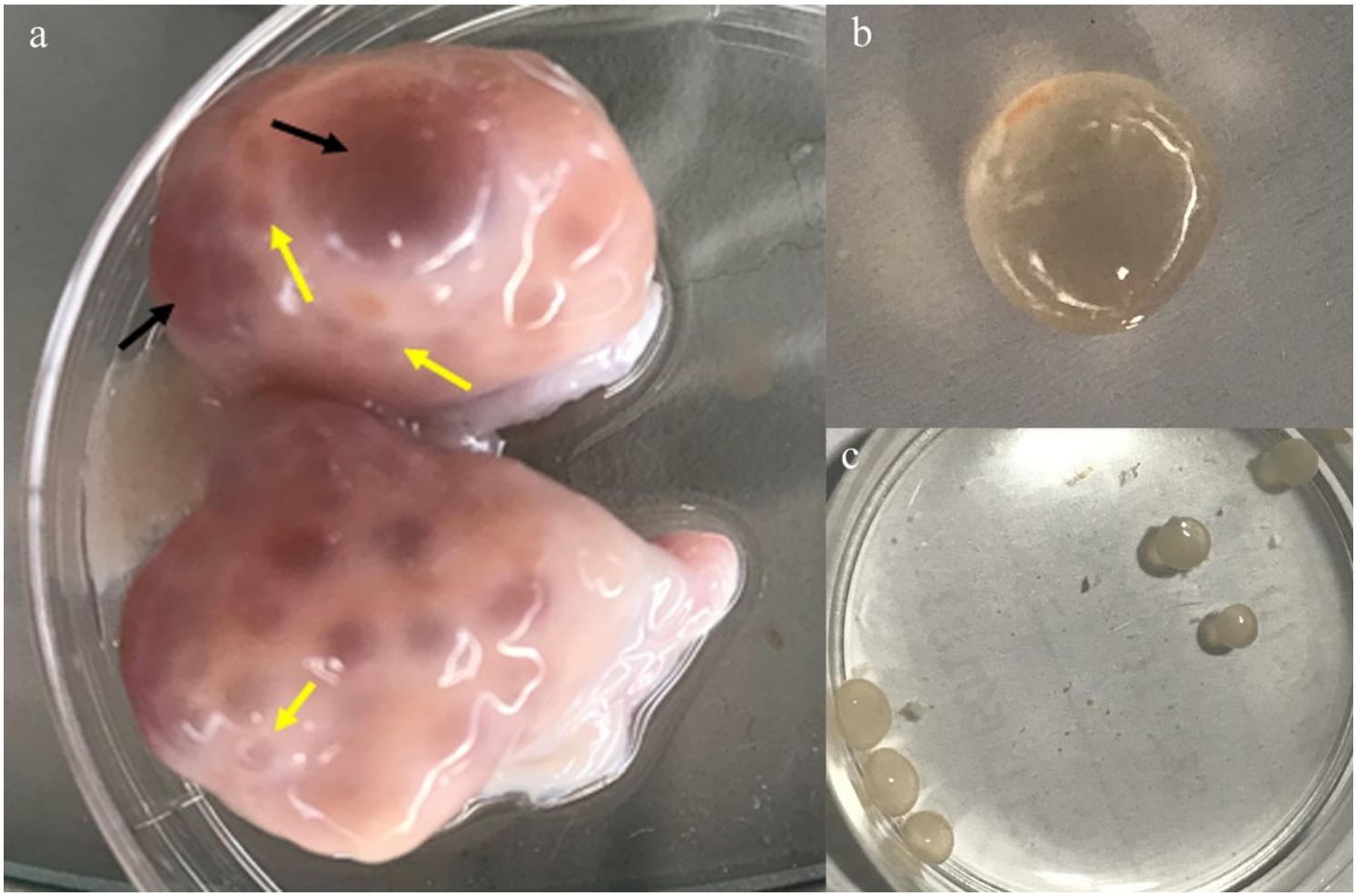

Figure 1

Pictures of ovaries and follicles. (a) Large follicles (black arrows) and small follicles (yellow arrows) in the ovaries before follicle separation. (b) large follicles after separation. (c) small follicles after separation.

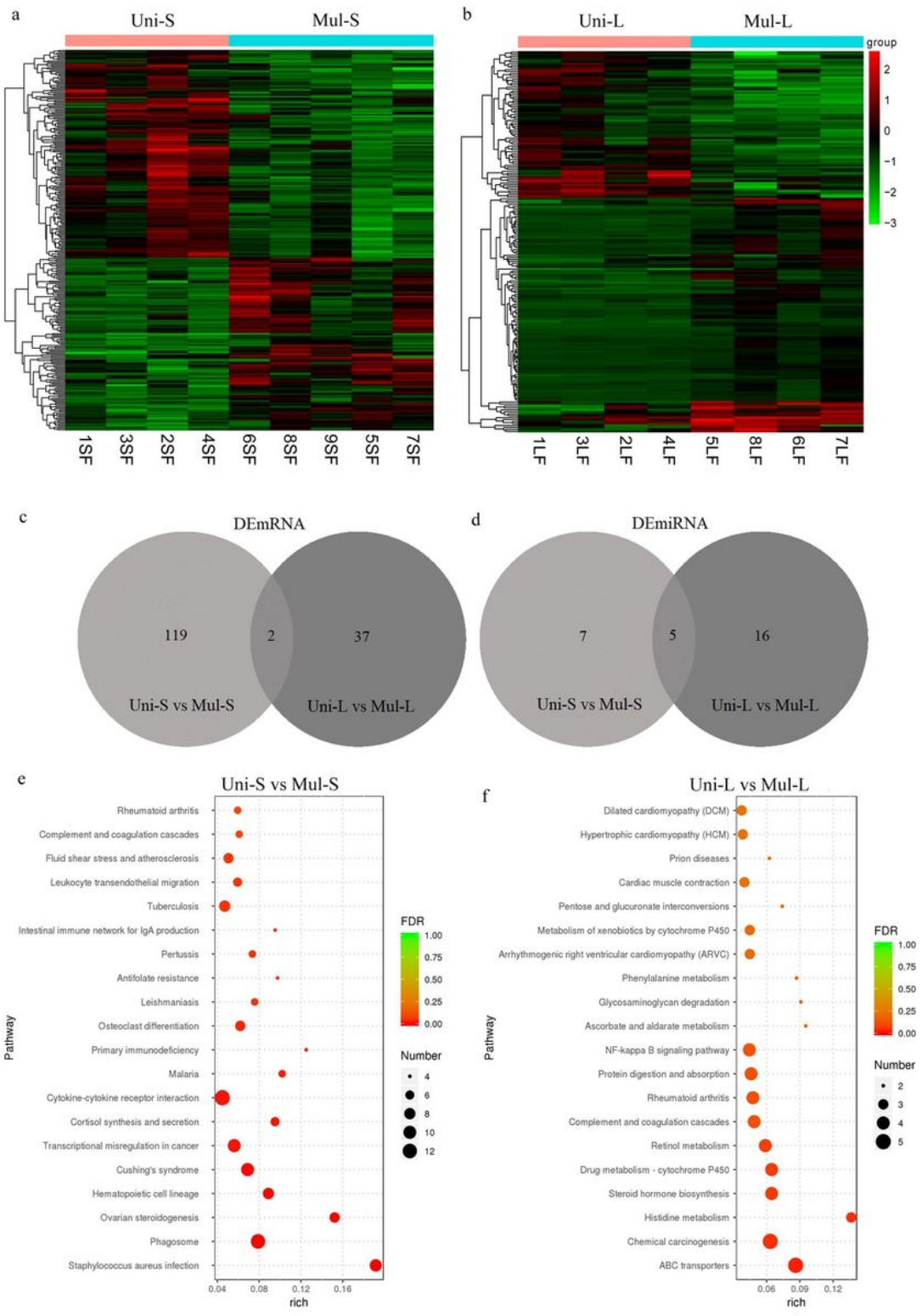

Figure 2

RNA-seq reveals distinct expression pattern of DEmRNAs on large and small follicles from uniparous and multiple goats. (a) Unsupervised clustering analysis showing expression profiles of DEmRNAs between Uni-S and Mul-S groups. (b) Unsupervised clustering analysis showing expression profiles of DEmRNAs between Uni-L and Mul-L groups. (c) Venn diagrams demonstrating the distribution of the DEmRNA shared in Uni-S vs Mul-S and Uni-L vs Mul-L groups. (d) Venn diagrams demonstrating the distribution of

the DEmiRNA shared in Uni-S vs Mul-S and Uni-L vs Mul-L groups, respectively. (e) Top ten KEGG pathways of DEmRNAs in the Uni-S vs Mul-S. (f) Top ten KEGG pathways of DEmRNAs in the Uni-S vs Mul-S (a) and Uni-L vs Mul-L (b)

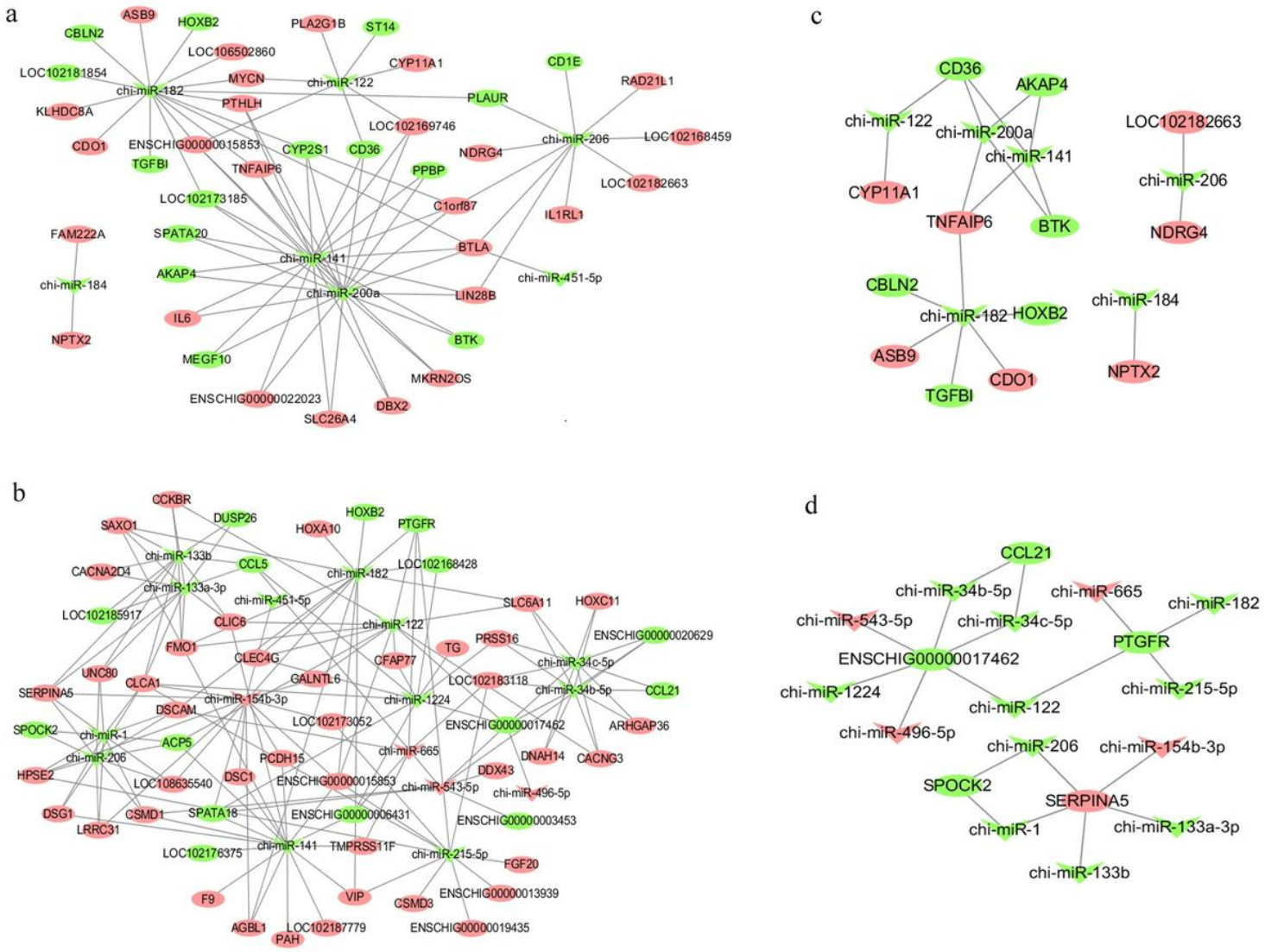

Figure 3

The original and selected DEmRNA-DEmiRNA interaction network of Uni-S vs Mul-S and Uni-L vs Mul-L. (a) The original DEmRNA-DEmiRNA interaction network of Uni-S vs Mul-S. (b) The original DEmRNA-DEmiRNA interaction network of Uni-L vs Mul-L. (c) The selected DEmRNA-DEmiRNA interaction network of Uni-S vs Mul-S. (d) The selected DEmRNA-DEmiRNA interaction network of Uni-L vs Mul-L. Ellipses and v shape represented DEmRNAs and DEmiRNAs, respectively. Red and green color of nodes represented upregulation and downregulation, respectively.

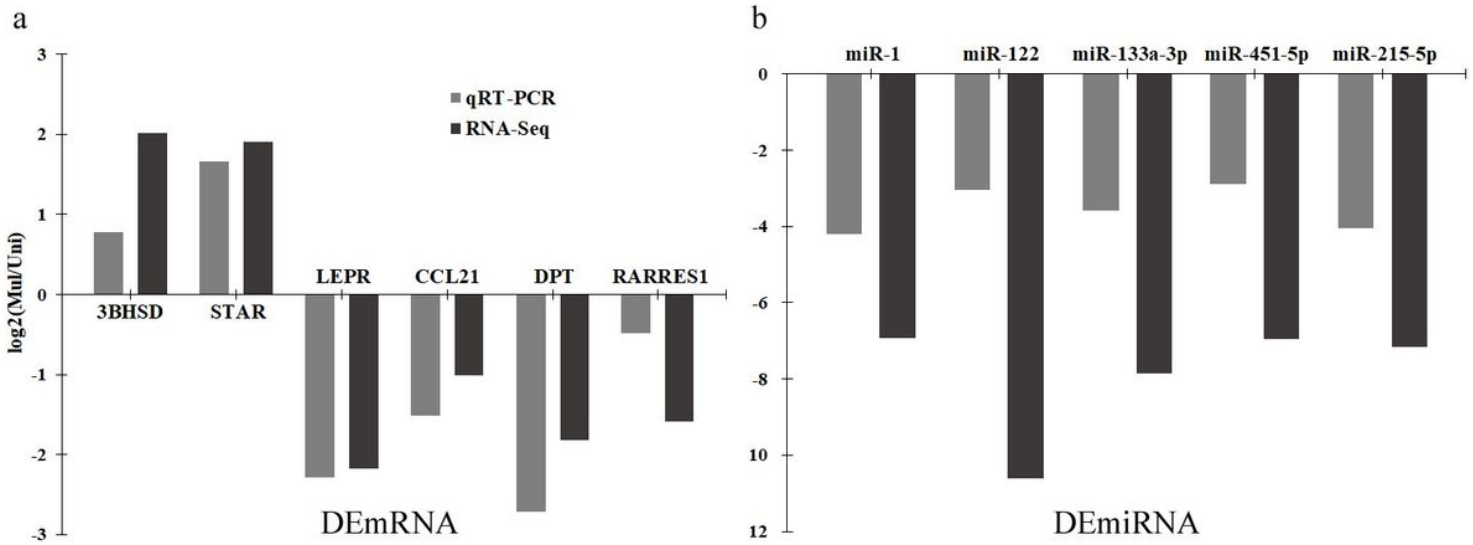

Figure 4

Verification of differently expressed genes and miRNAs by qRT-PCR. (a) The expression of six genes was validated using qRT-PCR and compared with the expression levels obtained from RNA-seq. (b) The expression of five miRNAs was validated using qRT-PCR and compared with the expression levels obtained from RNA-seq. Expression data are presented as expression values of genes and miRNAs in Uni-S vs Mul-S and Uni-L vs Mul-L. The qRT-PCR of genes values were normalized relative to the expression levels of Actin-β in the same cDNA sample, and miRNAs were relative to the expression levels of U6.